RAPID COMMUNICATIONS

PHYSICAL REVIEW B VOLUME 50, NUMBER 20 15 NOVEMBER 1994-II

High-resolution electron microscopy and inelastic light scattering of purified multishelled carbon nanotubes

W. S. Bacsa
Institut de Physique Expérimentale, Ecole Polytechnique Fédérale de Lausanne (EPFL), CH-1015 Lausanne, Switzerland

D. Ugarte
Laboratorio Nacional de Luz Sincrotron, Conselho Nacional de Desenvolvimento Científico e Technológico, Ministério da Ciência e Tecnologia, Caixa Postal 6192, 13081-970 Campinas, São Paulo, Brazil

A. Châtelain and W. A. de Heer
Institut de Physique Expérimentale, Ecole Polytechnique Fédérale de Lausanne (EPFL), CH-1015 Lausanne, Switzerland
(Received 5 August 1994)

Raman spectra of purified carbon deposits containing multishelled carbon nanotubes of average diameter 10–12 nm show narrow vibrational bands and no phonon softening in contrast to unpurified material. This is in agreement with lattice-dynamical calculations using a semiempirical pseudopotential, which predicts no significant phonon softening in this size range. Only a very weak disorder-induced vibrational band at 1356 cm^{-1} ($I_G/I_D=0.04$) is found for the unpurified as well as purified carbon deposits, which suggests that the scattering is originated by structural defects rather than by size effects.

Carbon nanotubes are unique in their structure in that they consist of concentric graphitic tubes with diameters of the order of several nanometers and several micrometers in length resulting in a large aspect ratio. The tubular structure and anisotropy of the curved graphene sheets are expected to give rise to unusual physical properties.[1] It has been experimentally found that carbon deposits generated on the electrodes of an arc discharge contain not only a large fraction of carbon nanotubes but also a large amount of multishelled often faceted graphitic nanoparticles.[2] Characterization of the unique macroscopic physical properties of nanotubes clearly requires purified materials. Ebbesen *et al.* have recently shown that nanotubes can be purified from carbon particles through oxidation at high temperature (750 °C).[3]

We have employed this oxidation purification scheme for the isolation of nanotubes and used phonon Raman spectroscopy to study the vibrational properties of purified nanotube samples. Raman spectroscopy is particularly useful to probe the microscopic structure averaged over a macroscopic sample volume. Raman spectra of unpurified carbon nanotubes have been reported earlier.[4] The in-plane stretching mode at 1582 cm^{-1} of graphite was found to be downshifted by 8 cm^{-1}. This phonon softening was thought to be a unique feature of the phonon spectrum of nanotubes.[4] However, closed-shell carbon particles show a similar downshifted phonon band.[5] The phonon softening in closed-shell carbon particles has been related to the spherical curvature of graphene sheets by lattice-dynamical calculations.[5] While the average closed-shell carbon particle size (4–7 nm) in Ref. 5 is smaller than the average tube diameter (10–20 nm) found in typical arc deposits and also, as curvature-induced phonon softening is expected to be less important for nanotubes than for spherical particles, we have examined in detail the phonon spectrum of purified nanotubes. Using high-resolution electron microscopy (HREM) to monitor the purification and to measure typical tube diameters and lengths, we recorded Raman spectra of purified and nonpurified deposits. In contrast to unpurified material, we found no phonon softening of the Raman-allowed phonon band at 1582 cm^{-1}. We show that this fact is consistent with lattice-dynamical calculations, which predict no significant phonon softening in the Raman spectrum of nanotubes in this size range (10–20 nm).

Carbon nanotubes have been synthesized in our laboratory in a conventional dc arc discharge (20 V, 80 A) in He atmosphere (350 mbar) using carbon electrodes of 6 mm diameter following the method suggested by Ebbesen and Ajayan.[2] The cylindrical deposit on the negative electrode with a light-gray-colored very hard outer surface layer, contained a soft black core. Scanning electron microscopy images of the soft black material consisting of mostly fibers of 100–200 μm diameter and lined parallel to the cylinder axis show loosely connected nanotubes. The black-core material has been purified following a three-step procedure: (a) the deposit has been dispersed in alcohol using ultrasonic agitation to isolate larger fragments, (b) centrifuged, and finally, (c) the solution with the dispersed material has been dried and annealed at 650 °C in air for 15 min. For HREM we used a 300-kV Philips EM430 microscope [Institut Interdepartemental de Microscopie Electronique (I^2M), EPFL] and Raman spectra were recorded at 514.5 nm and 5 mW with a Dilor spectrometer (Laboratoire de Metallurgie Physique) with a typical spot size of 0.2 mm.

Figure 1 shows HREM images of the unpurified [Fig. 1(a)] and purified [Fig. 1(b)] material. The large number of particles seen in the unpurified material is largely reduced after oxidation of 650 °C. It is found that most of the remaining smaller particles seen in the purified material are impurities introduced during the oxidation step. Larger remaining particles are found to be short, strongly oxidized nanotubes. The tube endings were found to be opened. The size distribution of the nanotubes before oxidation (Fig. 2) shows a maximum at 10–12 diameter.

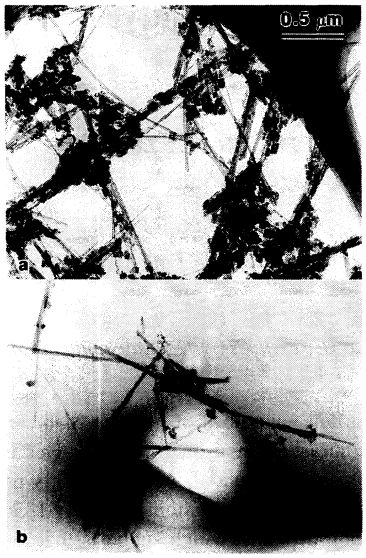

FIG. 1. HREM images of unpurified (a) and purified (b) carbon nanotubes of the same arc deposit.

Figure 3 shows the vibrational Raman spectra of purified and nonpurified carbon nanotubes of the sample shown in Fig. 1. Both spectra are very similar with a narrow Raman-allowed phonon peak at 1581 cm^{-1} with a weak shoulder extending to 1620 cm^{-1} and a disorder-induced band at 1356 cm^{-1}. The narrow linewidth and the low intensity of the disorder-induced peak indicates a high degree of graphitization and compares well with Raman spectra of pyrolytic graphite.[7] Table I shows the extracted line positions and peak widths of Lorentzian fits to the spectra shown in Fig. 3. For the purified material, one observes a slightly larger phonon energy and smaller peak width of the allowed Raman peak and also of the disorder-induced phonon band at 1356 cm^{-1}. The relative intensity of the disorder-induced vibrational band at 1355 cm^{-1} is found to be very small ($I_D/I_G=0.04$) for the unpurified, as well as for purified material. This peak is significantly smaller than in other published Raman spectra of unpurified nanotubes.[4,6] In disordered graphite the relative intensity is thought to be related to the average in-plane graphene size. The mixed-phase character of the arc discharge deposits, however, suggests that the relative intensity in unpurified deposits is dependent on details of the discharge process. We have observed more regular deposits and no gray inner inclusions if the discharge has been run in a stable regime (20 V, 80 A). The unchanged relative intensity of the 1350-cm^{-1} peak (within experimental error) for purified and unpurified deposits (Fig. 3) suggests that contributions from other forms of graphite present before the oxidation are not significant and that graphitic particles and nanotubes as observed in Fig. 1 contribute very little to scattering in the 1350-cm^{-1} energy range. Scattering in this energy range originates presumably from defects in the curved graphene sheets, tube ends, and remaining graphitic particles.

TABLE I. Raman peak positions, peak half-widths, and relative intensity $I_{D/G}$ ($I_{D/G}:=I_D/I_G$) of nonpurified and purified arc carbon deposit (Fig. 3).

	ω_G (cm^{-1})	$\Gamma_G/2$ (cm^{-1})	ω_D (cm^{-1})	$\Gamma_G/2$ (cm^{-1})	$I_{D/G}$
Error	±0.5	±0.5	±1.0	±2.0	±0.01
Nonpurified	1580.3	20.0	1356.0	39.0	0.03
Purified	1581.2	18.5	1356.0	31.0	0.04

For materials that contain a large number of graphitic carbon particles, we have observed, in the sequence of several measurements on different deposits and locations on the sample surface, a downshifted optical-phonon band (3–8 cm^{-1}). While this downshift can be seen by Raman spectroscopy, the very heterogenous particle and tube-size distribution of the carbon deposits revealed no apparent different average particle size in HREM images.

Figure 4 shows the second-order Raman spectrum of unpurified [Fig. 4(a)] and purified [Fig. 4(b)] carbon deposits. Apart from second-order scattering at 2450, 2700, and 3250 cm^{-1} also observed in pyrolitic graphite, one observes a narrow band at 2900 cm^{-1} for the purified material. Apart from a hydrogen-induced stretching vibration at 2800 cm^{-1}, a much broader vibrational band at 2950 cm^{-1} has been observed in more disordered forms of graphitic carbon.[8] Since the first-order vibrational spectrum of the purified material does not show enhanced disorder-induced scattering in the 1350-cm^{-1} energy range, it is concluded that the observed

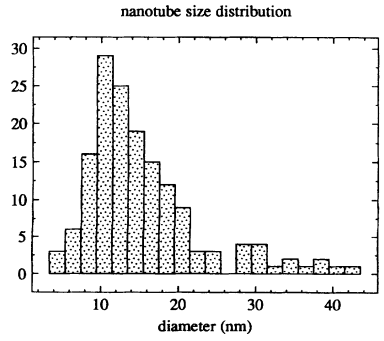

FIG. 2. Size distribution of carbon nanotubes shown in Fig. 1(a).

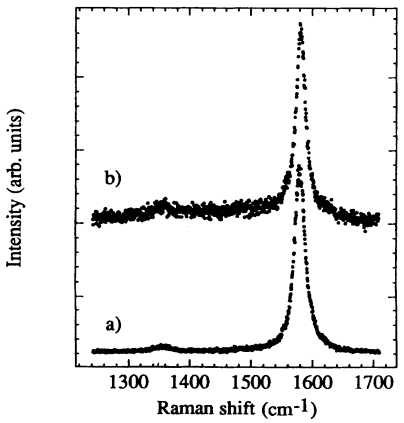

FIG. 3. Unpolarized first-order Raman spectrum of unpurified and purified carbon nanotubes. Same deposit as shown in Fig. 1.

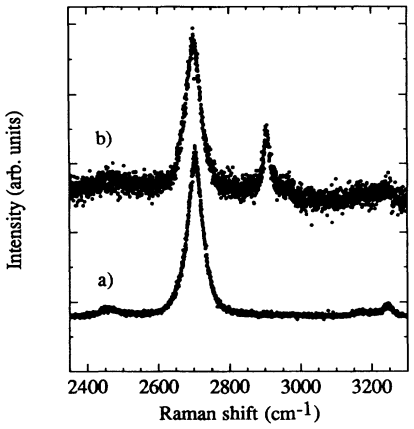

FIG. 4. Unpolarized second-order Raman spectrum of unpurified and purified carbon nanotubes. Same deposit as shown in Fig. 1.

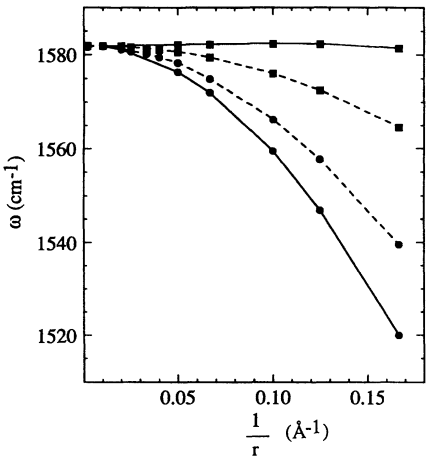

FIG. 5. Calculated zone-center optical-phonon energy in a single graphene sheet in function of radius of curvature for tubes with one of the bonds parallel (full lines) and perpendicular (dashed lines) to the tube axis. Within a pair of lines, the upper branch corresponds to a stretching vibration perpendicular (square) to the tube axis and the lower branch a stretching vibration parallel to the tube axis (circle).

vibrational band at 2900 cm^{-1} is due to hydrogen impurity (C-H stretch) introduced apparently during the high-temperature oxidation.

In order to estimate curvature-induced effects on the vibrational properties of graphene sheets, we have used the semiempirical interatomic Tersoff pseudopotential for carbon.[9] Although this pseudopotential is known to lead to overestimated optical-phonon energies compared to experimental values, it has the advantage that structural changes can be realistically implemented. Inclusion of only first-nearest neighbors simplifies the calculation even more. In order to obtain values that can be compared to experiments, the calculated values are linearly scaled to the experimental value for graphite. An analogous calculation had been carried out earlier for spherical carbon nanoparticles,[5] where the calculated phonon softening for smaller particle diameters is in excellent agreement with the average particle diameter as observed with HREM. Figure 5 shows the calculated phonon energy after minimizing the cohesive energy and solving the dynamical matrix for a single curved graphene sheet as a function of curvature radius. One of the bond directions in the honeycomb lattice has been chosen to lie parallel or perpendicular to the tube axis, which implies that the tube geometry considered for the calculation has no helical structure. The cylindrical curvature splits the twofold-degenerate in-plane phonon mode in graphite and induces softening of the optical phonon. The downshift is sizable for tubes with a few nm diameter (8–20 cm^{-1}) but is less than 1 cm^{-1} for tubes of 10 nm diameter. From the calculated eigenvectors it is found that the stretching vibration parallel to the tube axis is more sensitive to curvature than the stretching vibration perpendicular to the tube axis. This can be qualitatively explained by the curvature-induced bond-angle changes in direction of the eigenvector. For one set of bonds parallel to the tube axis, a bond-angle reduction in the direction of the eigenvector has the strongest effect on the phonon softening (Fig. 5). In contrast, an eigenvector perpendicular to the tube axis for bonds parallel to the tube axis has very little effect on the phonon energy (Fig. 5). Although the calculated values are thought to be more accurate for larger diameters, it is interesting to compare them with recent Raman spectra of single-shell carbon nanotubes of $\sim$1.2 nm diameter.[10,11] Single-shell carbon nanotubes within a matrix of disordered carbon show a peak at 1564 cm^{-1}, which has been tentatively assigned to the vibrational spectrum of single-shell nanotubes.[11] This assignment is in excellent agreement with the calculated phonon softening of a tube with one of the bonds perpendicular to the tube axis and with a diameter of 1.2 nm (Fig. 5). Multishelled carbon nanotubes contain tubes with different diameters that contribute to the Raman spectrum separately. However, the intensity of the Raman peak can be approximated by the number of bonds. Since the number of bonds is proportional to the tube radius, tubes with the largest radius will dominate the spectrum if the Raman cross section is assumed to be constant for different tube diameters. It is important to note that helicity in the tube structure changes the local bond angle and hence will affect the phonon energy, which results in helicity dependent softening and splitting of the in-plane optical phonons. Their energies are expected to lie between the values of the two geometries considered in Fig. 5.

We have attributed the phonon softening in closed-shell carbon particles and nanotubes to curvature-induced bond-angle deviations and found that these effects are not very large (<1 cm^{-1}) for particles or tubes with diameters larger than 10 nm. It is important to consider also other factors, such as changes in interlayer interactions, that might influence the vibrational spectrum. Due to the nature of vibrational modes at the Brillouin zone center, the small separation (6 cm^{-1}) of the in-plane Raman-active E_{2g2} mode (1582 cm^{-1}, out-of-phase motion) and the in-plane infrared-active E_{1u} mode (1588 cm^{-1}, in-phase motion) has been associated with the weak interlayer van der Waals interaction.[12] While no large interlayer interaction changes are expected for the tube sizes considered here, the corresponding phonon shifts are expected to be not larger than a few wave numbers.

Apart from curvature-induced effects that soften and split the in-plane optical-phonon mode, the evolution of the Ra-

man spectrum of nanotubes with changing radius depends on the following two main effects: (a) the nanoscale tube diameter confines the in-plane phonons to the graphene tube and hence the largest phonon wavelength perpendicular to the tube axis is limited, and (b) the much reduced Brillouin zone of the tube leads to folding of the phonon-dispersion branches, giving rise to a number of zone-center phonon modes. The size effect is small for larger tubes, since the phonon-dispersion branches are flat near the Brillouin-zone center and the tube circumference is much larger ($r>0.5$ nm) compared to the in-plane lattice constant (0.25 nm). For tubes with a large diameter the additional zone-center phonon modes have mostly a low symmetry resulting in very little scattering in the Raman spectrum. However, as the tube diameter decreases, contributions due to zone folding are expected to become more important. Similar phonon-confinement and phonon-folding effects have been investigated in detail in epitaxial semiconductor superlattices.[13] For nanotubes with a smaller diameter (5 nm) one expects first to see the splitting of the in-plane phonon mode and additional zone-center modes for tubes with the smallest diameter.

In summary, we have isolated graphitic nanotubes from nanoparticles through high-temperature oxidation.[3] The purity of nanotubes has been verified by HREM from which an average diameter of 10–12 nm has been found. Raman spectra of the purified nanotubes reveal no phonon softening, in contrast to some unpurified deposits that contained graphitic carbon particles. Small scattering at 1350 cm^{-1} is thought to originate more from defects in curved graphene layers and residual particles than from size-induced effects. High-temperature oxidation is found to lead to a narrow hydrogen-induced vibrational band. Lattice-dynamical calculations using a semiempirical pseudopotential[9] predict no phonon softening for tubes with 10 nm or larger diameters, which is in agreement with the experimental findings.

We are thankful for the invaluable support of Dr. P. Stadelmann of the Institut Interdepartemental de Microscopie Electronique (I^2M/EPFL), and we thank also Dr. E. Blank and Y. von Kaenel of the Laboratoire de Metallurgie Physique (LMPH/EPFL), and M. Fazan (IPE/EPFL) for experimental support. We acknowledge the financial support from the Swiss National Science Foundation.

[1] T. W. Ebbesen, Annu. Rev. Mater. Sci. **24**, 235 (1994).

[2] S. Iijima, Nature **345**, 56 (1991); T. W. Ebbesen and P. M. Ajayan, *ibid.* **358**, 220 (1992).

[3] T. W. Ebbesen, P. M. Ajayan, H. Hiura, and K. Tanigaki, Nature **367**, 519 (1994).

[4] H. Hiura, T. W. Ebbesen, K. Tanigaki, and H. Takahashi, Chem. Phys. Lett. **202**, 509 (1993).

[5] W. S. Bacsa, W. A. de Heer, D. Ugarte, and A. Chatelain, Chem. Phys. Lett. **211**, 346 (1993).

[6] J. Kastner, T. Pichler, H. Kuzmany, S. Curran, W. Blau, D. N. Weldon, M. Delamesiere, S. Draper, and H. Zandbergen, Chem. Phys. Lett. **221**, 53 (1994).

[7] D. S. Knight and W. B. White, J. Mater. Res. **4**, 385 (1989).

[8] R. J. Nemanich and S. A. Solin, Phys. Rev. B **20**, 392 (1979).

[9] J. Tersoff, Phys. Rev. B **37**, 6991 (1988).

[10] W. S. Bacsa *et al.* (unpublished).

[11] J. M. Holden, P. Zhou, X. Bi, P. C. Ecklund, S. Bandow, R. A. Jishi, K. D. Chowdhury, G. Dresselhaus, and M. S. Dresselhaus, Chem. Phys. Lett. **220**, 186 (1994).

[12] *Light Scattering in Solids III*, edited by M. Cardona and G. Güntherodt, Topics in Applied Physics Vol. 51 (Springer, Berlin, 1982).

[13] *Light Scattering in Solids V*, edited by M. Cardona and G. Güntherodt, Topics in Applied Physics Vol. 66 (Springer, Berlin, 1989).

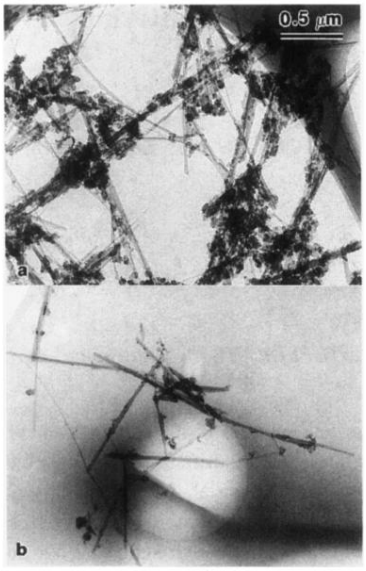

FIG. 1. HREM images of unpurified (a) and purified (b) carbon nanotubes of the same arc deposit.